doi:10.3788/gzxb20184705.0525002

# 六角密排多迭层碳纳米管阴极的大电子发射电流和高电子发射稳定性

李玉魁[1],刘云朋[2],武超[3],杨娟[1]

(1 金陵科技学院 电子信息工程学院,南京 211169)

(2 焦作大学 信息工程学院,河南 焦作 454000)

(3 中原工学院 电子信息学院,郑州 450007)

**摘 要**:研制了一种六角密排多迭层碳纳米管阴极.在这种结构中,衬底银电极由烧结的银浆制作在透明锡铟氧化物电极上,且具有六角形边缘,相邻衬底银电极交错排列于阴极面板上.用 ZnO 和 $SnO_2$ 颗粒作为掺杂材料,在衬底银电极和单一碳纳米管层之间制作了底部混杂层;单一碳纳米管层中的碳纳米管主要被用于发射阴极电子.给出了六角密排多迭层碳纳米管阴极的制作工艺,并研究了六角密排多迭层碳纳米管阴极用于电子源的可行性.将氮气作为保护气体,采用烧结方法除掉制备浆料中的有机粘合剂及其它有机杂质.将六角密排多迭层碳纳米管阴极真空密封进三极场发射显示器中,能够形成稳定的电子发射电流.测试结果表明,与普通碳纳米管阴极相比,六角密排多迭层碳纳米管阴极具有更优的电子发射特性,其开启电场为 1.83 V/μm,最大电子发射电流为 2 718.6 μA;且其具有良好的电子发射曲线趋势,当电场强度从 2.17 V/μm 增强到 3.06 V/μm 时,电子发射电流的增幅约为 1 410.3 μA.对电子发射电流随时间的波动变化进行了测试,测试结果显示六角密排多迭层碳纳米管阴极具有可靠且稳定的电子发射电流.绿色发射图像表明六角密排多迭层碳纳米管阴极具有良好的电子发射均匀性及高的电子发射亮度.鉴于其简单的制作结构和制作工艺,六角密排多迭层碳纳米管阴极具有一定的实际应用性.

**关键词**:碳纳米管阴极;制作工艺;发射电流;发射稳定性;银电极;结构

**中图分类号**:TB383; TB79 **文献标识码**:A **文章编号**:1004-4213(2018)05-0525002-9

# Large Electron Emission Current and High Electron Emission Stability of Hexagonal Close-packed Multi-lamination-layer Carbon Nanotube Cathode

LI Yu-kui[1], LIU Yun-peng[2], WU Chao[3], YANG Juan[1]

(1 *School of Electronic Information Engineering, Jinling Institute of Technology, Nanjing* 211169, *China*)

(2 *Department of Information Engineering, Jiaozuo University, Jiaozuo, Henan* 454000, *China*)

(3 *School of Electric and Information Engineer, Zhongyuan University of Technology, Zhengzhou* 450007, *China*)

**Abstract**: A Hexagonal Close-packed Multi-lamination-layer Carbon Nanotube (HCP-MLL-CNT) cathode is proposed. In this scheme, the silver slurry is sintered to form the substrate silver electrode with a hexagon-shaped edge, which is fabricated on the transparent indium-tin-oxide electrode, with a staggered arrangement of the adjacent substrate silver electrode on the cathode faceplate. Using ZnO and $SnO_2$ powders as mixing materials, the base blending layer is formed between the substrate silver

**Foundation item**: The National Natural Science Foundation of China (No.61302167), the Key Science and Technology Research Projects of Henan Province (No. 172102210390), and the Scientific Research Starting Foundation for High Level Talents in Jinling Institute of Technology (No.jit-rcyj-201602)

**First author**: LI Yu-kui (1973—), male, professor, Ph.D. degree, mainly focuses on flat panel display technology, electron device, solar cell fabrication, nano-materials preparation and applications. Email: lyksound@sina.com

**Received**: Nov.29, 2017; **Accepted**: Feb.05, 2018

electrode and the single CNT layer, whereas the CNTs in single CNT layers are mainly utilized to emit the cathode electrons. The fabrication process of an HCP-MLL-CNT cathode is discussed in detail, and and the feasibility study which the HCP-MLL-CNT cathode is applicable as an electron source is performed. The sintering method, in which the nitrogen gas is used as a protective gas, was adopted to remove the organic binder materials and other organic impurities of the preparation slurry. The HCP-MLL-CNT cathode was vacuum-sealed into the triode field emission display, and a stable electron emission current was formed. The measurement results indicate that the proposed HCP-MLL-CNT cathode possesses the enhanced electron emission characteristics, a low turn-on electric field of 1.83 V/$\mu$m, and the increased maximum electron emission current of 2718.6 $\mu$A. The HCP-MLL-CNT cathode revealed an excellent electron emission curve trend, in which the increasing range of electron emission current was approx. 1410.3 $\mu$A for the electric field enhancement range from 2.17 V/$\mu$m to 3.06 V/$\mu$m. The fluctuation of the electron emission current with time was also measured, and a reliable and stabile electron emission for HCP-MLL-CNT cathode was experimentally verified. The green emission image was displayed, which corroborated a good electron emission uniformity and high electron emission luminance of the proposed HCP-MLL-CNT cathode. It is shown that a simple fabrication structure and manufacturing process of the proposed HCP-MLL-CNT cathode possesses a high potential for practical applications.

**Key words**: Carbon nanotube cathode; Fabrication process; Emission current; Emission stability; Silver electrode; Structure

**OCIS Codes**: 250.0250; 230.2090; 230.4685; 350.5730; 230.4320

# 0 Introduction

Carbon Nanotubes (CNTs) are very promising for various field emitter applications, due to their unique characteristics of the concentric planar structure, nanoscale diameters, high mechanical strength, and superior chemical stability[1-3]. In vacuum environment, a mass supply of cathode electrons can be provided by CNTs to form a stable electron current[4-6]. Given this, CNTs have been successfully applied in the field emission display [7-9], and numerous studies on CNT cathodes were intensively conducted[10-12]. CNT cathodes are usually fabricated with the screen-printing process[13-15]. However, the most critical deficiency of printed CNT cathodes is their poor electron emission capability[16-18]. Therefore, various treatment techniques[19-21] including the plasma bombardment, ion irradiation, and mechanical rubbing methods have been applied to improve the field emission performance of CNT cathodes[22-24]. The plasma bombardment method could improve the emission uniformity of CNT cathode, but it was not suitable for the preparation of large-area CNT cathode. The ion irradiation method could enhance the electron emission ability of CNT cathode, however, the treatment cost was too expensive. The mechanical rubbing method was an effective technology, nevertheless, the CNT cathode surface usually was damaged[25-27]. Furthermore, an alternative solution to this problem was proposed by developing a new CNT cathode fabrication structure and the respective innovative CNT cathode preparation process[28-30]. In this study, a novel Hexagonal Close-packed Multi-lamination-layer CNT (HCP-MLL-CNT) cathode is explored. The design and fabrication of HCP-MLL-CNT cathode are described in detail, wherein the hexagonal close-packed substrate silver electrode was fabricated and the base blending layer was introduced between the hexagonal close-packed substrate silver electrode and the single CNT layer. The field emission display, in which the dot matrix image could be displayed, was fabricated, and its performance proved the feasibility of fabricated HCP-MLL-CNT cathodes. The electron emission characteristics were studied, and the electron emission current fluctuations were measured.

# 1 Experiment

## 1.1 Structure and design of CNT cathode

The structural schematic diagram of HCP-MLL-CNT cathode is shown in Fig. 1(a), and the commonly treated Indium-tin-oxide (ITO) electrode CNT cathode schematic structure is illustrated in Fig. 1(b). For the two types of CNT cathodes, the flat-panel soda-lime glass with a thickness of 2 mm was used to form the cathode faceplate. The HCP-MLL-CNT cathode, in which the multi-walled CNTs were

utilized as the electron emission materials, was fabricated on the cathode faceplate surface. The bar-shaped transparent ITO electrodes were fabricated with the etched ITO film. The substrate silver electrode, which was formed with the sintered silver slurry, was fabricated on the transparent ITO electrode, whereas the external edge of each substrate silver electrode had an interconnecting hexagonal shape. The schematic structure of the substrate silver electrode is illustrated in Fig.2. The single CNT layer was printed on the base blending layer.

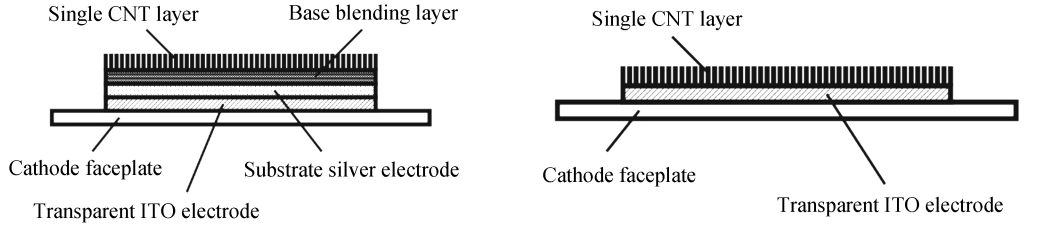


(a) Design of the HCP-MLL-CNT cathode (b) Structure of the commonly treated ITO electrode CNT cathode

Fig.1 Structural schematic diagram of two types of CNT cathodes

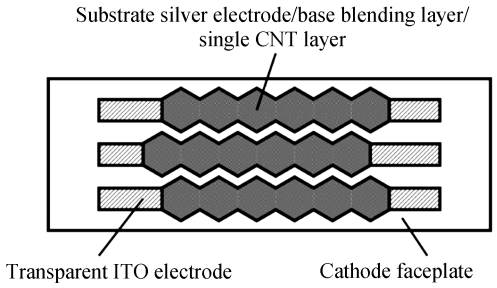


Fig.2 Design of substrate silver electrode in HCP-MLL-CNT cathode

### 1.2 Fabrication of HCP-MLL-CNT cathode

The total fabrication process of the HCP-MLL-CNT cathode can be roughly reduced to the three main steps. Firstly, with a high-precision photo-etching process, the ITO film covered on the cathode faceplate is split to form transparent ITO electrodes. The bar-shaped transparent ITO electrodes were serially arranged and separately insulated. The silver slurry was screen-printed on the cathode faceplate and subsequently sintered to form the substrate silver electrode. A satisfactory electrical conduction was achieved between the transparent ITO electrode and the substrate silver electrode. Secondly, two types of printing slurry, namely the single CNT layer slurry and the base blending layer slurry, were prepared. The purified multi-walled CNT, ZnO powder, and $SnO_2$ powder were blended to form a CNT-ZnO-$SnO_2$ mixture with the respective weight ratio of 1 : 0.5 : 0.5. Terpineol and ethyl cellulose were added to the above mixture, and the CNT-ZnO-$SnO_2$ mixture was thoroughly stirred with a magnetic stirrer at the temperature of 115℃ to form the base blending layer slurry. The purified multi-walled CNT, terpineol, and ethyl cellulose were mixed in the beaker. The single CNT layer slurry was obtained by a similar preparation process, which differed from the base blending layer slurry only by the stirring temperature (92℃). Thirdly, the base blending layer slurry was printed on the substrate silver electrode with the screen-printing method. The fabricated base blending layer slurry was baked in a special automatic oven at the constant baking temperature of 215℃. Subsequently, the baked base blending layer slurry on the substrate silver electrode was sintered in the nitrogen atmosphere in a special sintering furnace. The highest sintering temperature was 555℃, and the whole sintering time was approx. 60 min. So the base blending layer was fabricated. Then, the single CNT layer slurry was also printed on the base blending layer. A baking process for the fabricated single CNT layer slurry was performed to remove the organic additives, in which the constant baking temperature was 185℃. The corresponding sintering process for the baked single CNT layer slurry was conducted again in a special sintering furnace, of which the highest sintering temperature was also 555℃. Because the nitrogen was used as the protective gas, the CNT could not be oxidized in such a high sintering temperature environment. Finally, the proper post-treatment

process was performed for the single CNT layer to improve its electron emission, which concluded the HCP-MLL-CNT cathode fabrication.

### 1.3 Electron emission testing

For analyzing the CNT surface morphology of HCP-MLL-CNT cathode, Scanning Electron Microscopy (SEM) was employed, and the SEM images were also obtained. The triode field emission display with HCP-MLL-CNT cathode was fabricated, and the electron emission characteristics of HCP-MLL-CNT cathode were tested with a triode structure configuration. The DC operating voltages were applied for the triode field emission display, and the electron emission current was monitored with an ammeter.

To compare the influence of different CNT cathode on the electron emission characteristics, the other two CNT cathode samples, commonly treated ITO electrode CNT cathode and non-oxidation sintered HCP CNT cathode, were also fabricated with a similar manufacturing process. The single CNT layer slurry was printed directly on the transparent ITO electrode surface, so the commonly treated ITO electrode CNT cathode was prepared. The fabrication structures of the non-oxidation sintered HCP CNT cathode, and the HCP-MLL-CNT cathode are the same, the only difference being in their fabrication processes, where the highest sintering temperature was 332℃ for the non-oxidation sintered HCP CNT cathode.

## 2 Results and discussion

### 2.1 SEM images of CNT cathode

Fig.3 presents the SEM images of three types of CNT cathode samples. The magnification factor of all the three SEM images, which was 30 000, was identical, and the surface morphology of CNT cathode can be observed.

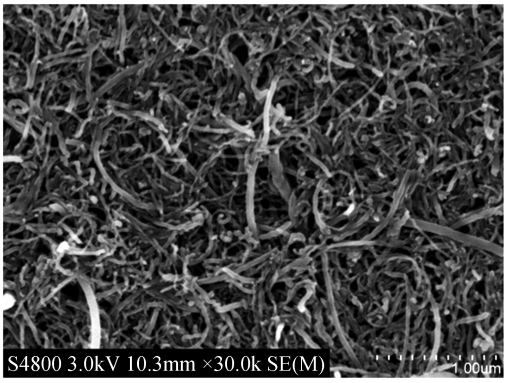


(a) SEM image of the commonly treated ITO electrode CNT cathode

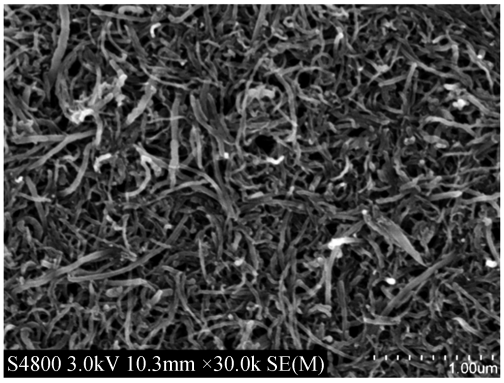


(b) SEM image of the HCP-MLL-CNT cathode

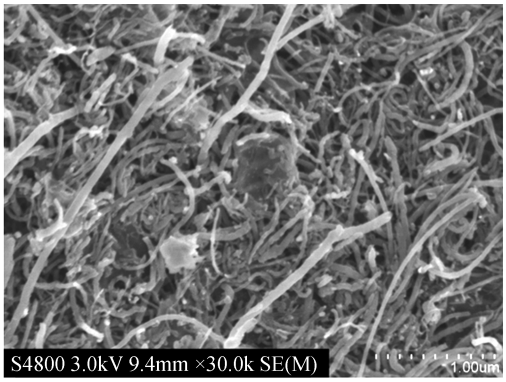


(c) SEM image of the non-oxidation sintered HCP CNT cathode

Fig.3 Surface morphology of three types of CNT cathodes

As shown in Fig.1(a), nubbly organic binder materials, which covered the surface of commonly treated ITO electrode CNT cathode, have disappeared. Many CNT ends protruded from CNT cathode surface, which would form potential electron emission sites. The HCP-MLL-CNT cathode is shown in Fig.

3(b). As seen from the image, numerous CNT ends were irregularly distributed along the CNT cathode surface, the organic contaminants had been removed entirely, and a clean and homogeneous cathode surface was achieved, which should be favorable to enhance the electron emission current of the HCP-MLL-CNT cathode. In fact, in the commonly treated ITO electrode CNT cathode, the single CNT layer was fabricated on the transparent ITO electrode; and in the HCP-MLL-CNT cathode, the single CNT layer was also prepared on the base blending layer. For the two types of CNT cathode, seen from the fabrication structure, the same single CNT layers were manufactured at the top of CNT cathode; seen from the main cathode function, the same single CNT layers were utilized to emit adequate cathode electrons. So, it was no surprising that both types of CNT cathode possessed identical and good cathode surfaces.

For the HCP-MLL-CNT cathode, a smooth cathode surface was composed of pure CNTs. It was ensured that all the acquired cathode electrons should be emitted by the CNTs. In the contact interface of the single CNT layer and the base blending layer, after the sintering treatment, parts of CNTs in the two CNT layers were interpenetrated, and an improved interface contact was formed. However, due to the covered single CNT layer, no ZnO and $SnO_2$ particles appeared on the cathode surface. Moreover, all the organic impurities and solvent could not be observed at the cathode surface, which also implied that the sintering for HCP-MLL-CNT cathode was complete in the sintering process; many CNTs were preserved on the cathode surface, which proved the shielding action of nitrogen gas.

In the course of HCP-MLL-CNT cathode preparation, the high-temperature sintering method was used, in which the nitrogen gas of 99.999% purity was employed in the sintering environment, while the highest sintering temperature was 555℃. The sintering method was a non-contact treatment process, which was more suitable for the fabrication of large-area CNT cathode. Moreover, the CNT cathode surface would not be exposed to a direct contact in the treatment course, so the mechanical damaging would be avoided, and the contamination of other foreign residues would not emerge. On the one hand, the sintering temperature was high. Because the oxygen was excluded from contact with CNTs in the HCP-MLL-CNT cathode, no oxidation occurred; meanwhile, the CNT could also endure a high sintering in the nitrogen atmosphere. In other words, the CNT in HCP-MLL-CNT cathode was undamaged in the sintering course. However, the organic binder materials and other impurities in the cathode slurry were fully evaporated. On the contrary, if the sintering temperature was low, the treatment result might be unsatisfactory. One more SEM image of non-oxidation sintered HCP CNT cathode is depicted in Fig.3(c). In this experiment, the sintering process was also carried out: the highest sintering temperature was 332℃, in contrast to the normal sintering temperature of 555℃. As seen from the above image, after the non-oxidation sintering treatment, there was still some organic binder materials at the CNT cathode surface, although their blocks had been eliminated. This implies that the removal process of organic binder materials was incomplete. As compared to clean and homogeneous surface of the HCP-MLL-CNT cathode, that of non-oxidation sintered HCP CNT cathode contained the residual materials, which would interfere with the protrusion of CNTs and strongly restrain their electron emission capabilities. Therefore, the appropriate treatment temperature is crucial for the HCP-MLL-CNT cathode fabrication by the sintering method. On the other hand, in the sintering process, the continuously provided nitrogen gas was flowing at a constant rate. With the gas flow of nitrogen, the organic binder materials in HCP-MLL-CNT cathode would be sintered thoroughly. Not only the re-deposition of residual organic binder materials was excluded, but also the transformation of organic impurities was thus prevented.

### 2.2 Electron emission characteristic curves

Measurements of electron emission characteristics of two types of CNT cathode samples, namely the commonly treated ITO electrode CNT cathode and the HCP-MLL-CNT cathode, were carried out in a vacuum chamber of $10^{-4}$ Pa, and the respective electron emission curves are plotted in Fig. 4. For the characteristics' measurement, the HCP-MLL-CNT cathode was assembled in the vacuum chamber of one field emission display, while the commonly treated ITO electrode CNT cathode was installed in another field emission display, and the corresponding test curves are depicted in Fig.4, respectively. Insofar as the electron emission properties were quite poor, the assembling and measuring of non-oxidation sintered HCP

CNT cathode sample was abandoned. In the measuring course, two DC operating voltages, namely the anode bias voltage and the grid bias one, were applied. The anode bias voltage of 1.73 kV remained constant for both types of CNT cathode samples.

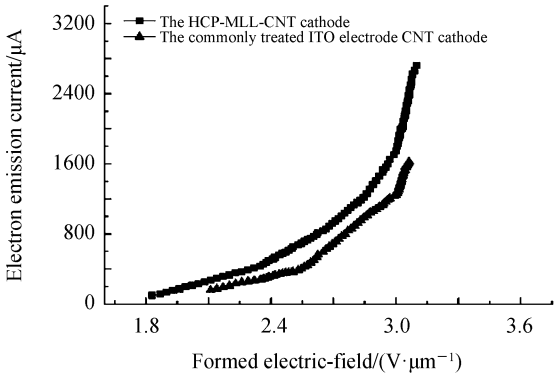


Fig.4 Electron emission characteristic curves for two types of CNT cathodes

As expected, in comparison with the commonly treated ITO electrode CNT cathode, the HCP-MLL-CNT cathode exhibited significantly improved electron emission properties, judging from the following three aspects. Firstly, the HCP-MLL-CNT cathode possessed a lower turn-on electric field of 1.83 V/μm, as compared to that of commonly treated ITO electrode CNT cathode, which attained 2.11 V/μm, so that the respective difference made about 0.28 V/μm. This strongly suggests that the HCP-MLL-CNT cathode would emit cathode electrons more readily than the commonly treated ITO electrode CNT cathode. The fabrication of base blending layer is the most critical for improving the HCP-MLL-CNT cathode performance. In the base blending layer, ZnO and $SnO_2$ particles penetrated into the space of CNT which was twined each other. Due to different sizes of ZnO and $SnO_2$ particles, the CNT cathode surface roughness was increased; due to the efficient separating of ZnO and $SnO_2$ particles in dense CNTs, the local electric field of each CNT emitter was enhanced, and the electric field enhance factor was also improved. These measures were quite instrumental in reducing the turn-on electric field of the HCP-MLL-CNT cathode. Secondly, the HCP-MLL-CNT cathode had a larger electron emission current. The maximum electron emission current of commonly treated ITO electrode CNT cathode was approx. 1623.8 μA, which was less than that of the HCP-MLL-CNT cathode (about 2718.6 μA). Meanwhile, with the same electric field of 2.83 V/μm, the electron emission current of HCP-MLL-CNT cathode reached 1187.2 μA, and that of commonly treated ITO electrode CNT cathode was about 956.4 μA. Thus, the HCP-MLL-CNT cathode could supply more cathode electrons in the normal operating course of field emission display. With large electron emission current, brightness and luminous efficiency of the field emission display with HCP-MLL-CNT cathode could be improved, as well as its luminance uniformity. Thirdly, the HCP-MLL-CNT cathode revealed a better electron emission curve trend. For example, when the electric field was enhanced from 2.71 V/μm to 3.06 V/μm, the increasing range of electron emission current for HCP-MLL-CNT cathode was approx. 1410.3 μA, while that of electron emission current for commonly treated ITO electrode CNT cathode was about 896.7 μA. As compared to commonly treated ITO electrode CNT cathode, the electron emission curve of the HCP-MLL-CNT cathode was steeper. One can conclude that the substrate silver electrode design with an HCP shape was beneficial for enforcing the CNT to emit more cathode electrons. The substrate silver electrode was inserted between the base blending layer and the transparent ITO electrode, and the staggered arrangement of the adjacent substrate silver electrodes was realized. For one substrate silver electrode, the electrode edge length was reasonably increased, which was expedient for the formation of a more robust CNT emitter. Moreover, given the further enhancement of the electric field at the electrode edge, it would be reasonable to assume that large electron emission current would be formed in HCP-MLL-CNT cathode at the same operating voltage. Also, due to a solid electric contact between the substrate silver electrode and transparent ITO electrode, the cathode potential conduction is also improved.

### 2.3 Emission image

For measuring and verifying the electron emission characteristics ofthe HCP-MLL-CNT cathode, the triode field emission display was vacuum-sealed. The monochrome anode was formed on the anode faceplate, wherein the green phosphor was prepared on the anode ITO electrode so that only a green image could be displayed. The HCP-MLL-CNT cathode was mounted onto the cathode faceplate. After the anode and cathode faceplate were combined to make a vacuum chamber, the HCP-MLL-CNT cathode was placed in the vacuum environment. The photograph of fully sealed field emission display is presented in Fig.5. The

small field emission display could display some dot matrix image. Due to the obscuring of other field emission display components, the HCP-MLL-CNT cathode is not visible from the field emission display exterior. Some specifications of the small field emission display were as follows. The external length/width dimensions were 160 mm and 50 mm, respectively. The anode and cathode faceplates had the same thickness of 2 mm. The anode faceplate contained 70 emission image pixels, which were subdivided into two groups. In each group , the emission image pixels were arranged into a 5 (line)×7 (column) matrix form. Each emission image pixel had the identical square shape and the area of 850 μm ×850 μm.

Fig.5 Photograph of fully-sealed field emission display with HCP-MLL-CNT cathode

Fig.6 shows the emission images of two types of CNT cathodes, respectively. As is seen from the emission images, the proper luminescence of all emission image pixels corroborates that both types of CNT cathodes can be applied to field emission display. Under the appropriate vacuum conditions, the HCP-MLL-CNT cathode is applicable as an electron source.

The emission image of commonly treated ITO electrode CNT cathode is presented in Fig.6(a). In general, the emission image luminance was non-uniform, of which some emission image pixels had grown brighter. On the contrary, as shown in Fig.6(b), all the emission image pixels were luminous, and the light intensity of each emission image pixels was nearly the same, while the brightness of emission image was quite high. In contrast to the commonly treated ITO electrode CNT cathode, the HCP-MLL-CNT cathode exhibited better electron emission characteristics, such as high electron emission luminance and good electron emission uniformity. On the one hand, in the HCP-MLL-CNT cathode, the substrate silver electrode featured two hexagon-shape electrode edges, while the adjacent substrate silver electrode had a staggered arrangement on the cathode faceplate. On the other hand, the substrate silver electrode was fabricated on the bar transparent ITO electrode, while an additional base blending layer was inserted between the substrate silver electrode and the single CNT layer. Thus, a multi-lamination-layer structure of CNT cathode was designed and successfully implemented. In the fabrication process, the HCP-MLL-CNT cathode was subjected to several high-temperature sintering procedures, which did not hinder its cathode electron emission performance. This finding corroborated the feasibility of the proposed fabrication method of the HCP-MLL-CNT cathode. The manufacturing cost is low, and the manufacturing process is relatively simple, which advantages are combined with an expected high reproducibility of the HCP-MLL-CNT cathode.

(a) Emission image of the commonly treated ITO electrode CNT cathode (b) Emission image of The HCP-MLL-CNT cathode

Fig.6 Emission images comparing of two types of CNT cathodes

### 2.4 Fluctuation curves of electron emission current with time

Fig.7 presents the typical fluctuation curves of electron emission current with time for the commonly treated ITO electrode CNT cathode and the HCP-MLL-CNT cathode. In this experiment, the anode bias voltage of 1.67 kV was fixed, and an initial electron emission current of 836.7 μA was set. The corresponding electron emission current was continuously monitored with an ammeter. As is seen from the

fluctuation curve trend, the electron emission current of both types of CNT cathodes firstly grew and then decreased.

In one respect, noteworthy is that the maximum electron emission current fluctuation rate of the HCP-MLL-CNT cathode was less than 5%, while that of commonly treated ITO electrode CNT cathode reached 12.4% in the measuring course. This fact strongly indicates the superiority of HCP-MLL-CNT cathode over the commonly treated ITO electrode CNT cathode by its electron emission current stability. In another respect, as shown in Fig.7, the commonly treated ITO electrode CNT cathode exhibited a more drastic change in the electron emission current than the proposed HCP - MLL - CNT cathode , which has a relatively smooth and monotonic fluctuation curve depicted. In other words, the electron emission current of the HCP-MLL-CNT cathode longer rise and fall periods, which implies that it is more reliable than the commonly treated ITO electrode CNT cathode. With an increase in the measurement period, the electron emission current variation of the HCP-MLL-CNT cathode was still quite small. As it was already mentioned, the HCP-MLL-CNT cathode possesses a homogeneous cathode surface and an additional fabricated base blending layer, which improvements ensure its electron emission current stability.

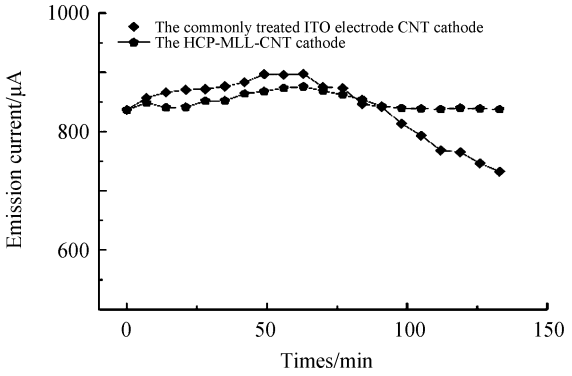


Fig.7 Fluctuation curves of electron emission current with time for two types of CNT cathodes

## 3 Conclusion

In this study, a simple fabrication process for HCP-MLL-CNT cathode was described in detail, and the feasibility studies on its practical applications were also performed. With sintered silver slurry, the substrate silver electrode was formed on the transparent ITO electrode, which edges had a hexagonal shape. Using ZnO and $SnO_2$ powders as mixing materials, the base blending layer was fabricated under the single CNT layer, while the CNTs in the single CNT layer were mainly used as the electron source. In the manufacturing process, the sintering method was adopted to remove the organic binder material and other organic impurities. It was proved that the HCP-MLL-CNT cathode was superior to the commonly treated ITO electrode CNT cathode by the electron emission characteristics (turn-on electric field of 1.83 V/μm versus 2.11 V/μm, the maximum electron emission current of 2718.6 μA versus 1623.8 μA), and by the electron emission curve trend. Furthermore, the performed measurements of the electron emission current fluctuation curves corroborated the stability and reliability of the HCP-MLL-CNT cathode. A field emission display with HCP-MLL-CNT cathode was fabricated, and a green emission image was exhibited, which proved the proposed HCP-MLL-CNT cathode applicability to field emission display. The new structure also appears to possess a high potential for practical applications.

**References**

[1] TRUONG T K, LEE Y, SUH D. Multifunctional characterization of carbon nanotube sheets, yarns, and their composites[J]. *Current Applied Physics*, 2016, **16**(9): 1250-1258.

[2] BULLER S, HEISE-PODLESKA M, PFANDER N, *et al*. Carbon nanotubes as conducting support for potential Mn-oxide electrocatalysts: lnfluences of pre-treatment procedures[J]. *Journal of Energy Chemistry*, 2016, **25**(2): 265-271.

[3] MALLAKPOUR S, ZADEHNAZARI A. Preparation of dopamine-functionalized multi-wall carbon nanotube/ poly (amide-imide) composites and their thermal and mechanical properties[J]. *New Carbon Materials*, 2016, **31**(1): 18-30.

[4] AAZAM E S. Visible light photocatalytic degradation of thiophene using Ag-$TiO_2$/ multi-walled carbon nanotubes nanocomposite[J]. *Ceramics International*, 2014, **40**(5): 6705-6711.

[5] DHIMAN S, KUMAR R, DHARAMVIR K. Study of structural and electronic properties of doped arm chair single-walled carbon nanotube[J]. *Materials Today: Proceedings*, 2016, **3**(6): 1820-1827.

[6] SAMIEE L, SHOGHI F, MAGHSODI A. In situ functionalization of mesoporous carbon electrodes with carbon nanotubes for proton exchange membrane fuel-cell application[J]. *Materials Chemistry and Physics*, 2014, **143**(3): 1228-1235.

[7] KANDASAMY R, MUHAIMIN I, MOHAMMAD R. Single walled carbon nanotubes on MHD unsteady flow over a

porous wedge with thermal radiation with variable stream conditions[J]. *Alexandria Engineering Journal*, 2016, **55**(1): 275-285.

[8] KWAK E H, YOON K B, JEONG G H. Comparative study on diameter distribution of single-walled carbon nanotubes using growth templates with different pore sizes: Zeolite-L, ZSM-5, and MCM-41[J]. *Current Applied Physics*, 2014, **14**(12): 1633-1638.

[9] MAITY S, DAS N S, SANTRA S, *et al*. CdS nanoparticle coated carbon nanotube through magnetron sputtering and its improved field emission performance[J]. *Current Applied Physics*, 2016, **16**(10): 1293-1302.

[10] HSIEH C T, GU J L, TZOU D Y, *et al*. Microwave deposition of Pt catalysts on carbon nanotubes with different oxidation levels for formic acid oxidation[J]. *International Journal of Hydrogen Energy*, 2013, **38**(25): 10345-10353.

[11] KAVINKUMAR T, MANIVANNAN S. Synthesis, characterization and gas sensing properties of grapheme oxide-multiwalled carbon nanotube composite[J]. *Journal of Materials Science & Technology*, 2016, **32**(7): 626-632.

[12] KWAK J H, HAN J K, KANG S W, *et al*. Dielectric relaxation properties of Pb $TiO_3$-multiwalled carbon nanotube composites prepared by a sol-gel process[J]. *Ceramics International*, 2016, **42**(7): 8165-8169.

[13] DARBARI S. Model calculation and empirical investigation of enhanced field emission behavior of branched carbon nanostructures[J]. *Current Applied Physics*, 2014, **14**(8): 1092-1098.

[14] HAYAT T, HUSSAIN Z, ALSAEDI A, *et al*. Carbon nanotubes effects in the stagnation point flow towards a nonlinear stretching sheet with variable thickness[J]. *Advanced Powder Technology*, 2016, **27**(4): 1677-1688.

[15] YOUH M J, CHOU Y P, LIU Y M, *et al*. Simulation and modeling of alignment-free field emission X-ray tubes[J]. *Applied Mathematical Modelling*, 2015, **39**(19): 5896-5906.

[16] SMITHSON C, WU Y, WIGGLESWORTH T, *et al*. Using unsorted single-wall carbon nanotubes to enhance mobility of diketopyrrolopyrrole-quarterthiophene copolymer in thin-film transistors[J]. *Organic Electronics*, 2014, **15**(11): 2639-2646.

[17] SARWAR M S U, DAHMARDEH M, NOJEH A, *et al*. Batch-mode micropatterning of carbon nanotube forests using UV-LIGA assisted micro-electro-discharge machining[J]. *Journal of Materials Processing Technology*, 2014, **214**(11): 2537-2544.

[18] THOMAS T, MASCARENHAS R J, MARTIS P, *et al*. Multi-walled carbon nanotube modified carbon paste electrode as an electrochemical sensor for the determination of epinephrine in the presence of ascorbic acid and uric acid[J]. *Materials Science and Engineering: C*, 2013, **33**(6): 3294-3302.

[19] SARASWAT S K, PANT K K. Synthesis of carbon nanotubes by thermo catalytic decomposition of methane over Cu and Zn promoted Ni/MCM-22 catalyst[J]. *Journal of Environmental Chemical Engineering*, 2013, **1**(4): 746-754.

[20] GKIKAS M, DAS B P, TSIANOU M, *et al*. Surface initiated ring-opening polymerization of L-proline N-carboxy anhydride from single and multi walled carbon nanotubes[J]. *European Polymer Journal*, 2013, **49**(10): 3095-3103.

[21] ROSADO G, VERDE Y, VALENZUELA-MUNIZ A M, *et al*. Catalytic activity of Pt-Ni nanoparticles supported on multi-walled carbon nanotubes for the oxygen reduction reaction[J]. *International Journal of Hydrogen Energy*, 2016, **41**(48): 23260-23271.

[22] ANGULAKSHMI V S, RAJASEKAR K, SATHISKUMAR C, *et al*. Growth of vertically aligned carbon nanotubes on a silicon substrate by a spray pyrolysis method[J]. *New Carbon Materials*, 2013, **28**(4): 284-287.

[23] WONG W Y, DAUD W R W, MOHAMAD A B, *et al*. Influence of nitrogen doping on carbon nanotubes towards the structure, composition and oxygen reduction reaction[J]. *International Journal of Hydrogen Energy*, 2013, **38**(22): 9421-9430.

[24] DJOKIC V R, MARINKOVIC A D, ERSEN O, *et al*. The dependence of the photocatalytic activity of $TiO_2$/ carbon nanotubes nanocomposites on the modification of the carbon nanotubes[J]. *Ceramics International*, 2014, **40**(3): 4009-4018.

[25] WANG Feng-ge, LI Yu-kui, LU Wen-ke. Fabrication of groove shape cold cathode forenhancing field emission properties of carbon nanotube[J]. *Acta Photonica Sinica*, 2014, **43**(4): 423001-423007.

[26] YOON D H, CHOI Y C. Improved field emission stability and uniformity of printed carbon nanotubes prepared using high energy-milled glass frit[J]. *Current Applied Physics*, 2013, **13**(7): 1477-1481.

[27] LI Yu-kui, WANG Feng-ge, LIU Xing-hui, *et al*. Fabrication of integral type cold cathode with carbon nanotube for improving the electrical contact and adhesion performance[J]. *Acta Photonica Sinica*, 2013, **42**(6): 637-644.

[28] BAEG K J, JEONG H J, JEONG S Y, *et al*. Enhanced ambipolar charge transport in staggered carbon nanotube field-effect transistors for printed complementary-like circuits[J]. *Current Applied Physics*, 2017, **17**(4): 541-547.

[29] TUNCKOL M, HEMANDEZ E Z, SARASUA J R, *et al*. Polymerized ionic liquid functionalized multi-walled carbon nanotubes/ polyetherimide composites[J]. *European Polymer Journal*, 2013, **49**(12): 3770-3777.

[30] AYKUT Y. Electrospun MgO-loaded carbon nanofibers: enhanced field electron emission from the fibers in vacuum[J]. *Journal of Physics and Chemistry of Solids*, 2013, **74**(2): 328-337.